DISCLAIMER

This report was prepared as an account of work sponsored by an agency of the United States Government. Neither the United States Government nor any agency thereof, nor any of their employees, makes any warranty, express or implied, or assumes any legal liability or responsibility for the accuracy, completeness, or usefulness of any information, apparatus, product, or process disclosed, or represents that its use would not infringe privately owned rights. Reference herein to any specific commercial product, process, or service by trade name, trademark, manufacturer, or otherwise does not necessarily constitute or imply its endorsement, recommendation, or favoring by the United States Government or any agency thereof. The views and opinions of authors expressed herein do not necessarily state or reflect those of the United States Government or any agency thereof. Reference herein to any social initiative (including but not limited to Diversity, Equity, and Inclusion (DEI); Community Benefits Plans (CBP); Justice 40; etc.) is made by the Author independent of any current requirement by the United States Government and does not constitute or imply endorsement, recommendation, or support by the United States Government or any agency thereof.

Pacific Northwest
NATIONAL LABORATORY

PNNL-35722

Monitoring of Photovoltaic (PV) Performance and Degradation

Integrated Renewable Energy Systems (IRES)

PV Monitoring Task

February 2024

Donghui Li
Jiyoung Son
Yelin Ni
Leo Fifield

U.S. DEPARTMENT OF ENERGY
Prepared for the U.S. Department of Energy
under Contract DE-AC05-76RL01830

DISCLAIMER

PACIFIC NORTHWEST NATIONAL LABORATORY
operated by
BATTELLE
for the
UNITED STATES DEPARTMENT OF ENERGY
under Contract DE-AC05-76RL01830

Printed in the United States of America

Available to DOE and DOE contractors from
the Office of Scientific and Technical Information,
P.O. Box 62, Oak Ridge, TN 37831-0062
www.osti.gov
ph: (865) 576-8401
fox: (865) 576-5728
email: reports@osti.gov

Available to the public from the National Technical Information Service
5301 Shawnee Rd., Alexandria, VA 22312
ph: (800) 553-NTIS (6847)
or (703) 605-6000
email: info@ntis.gov
Online ordering: http://www.ntis.gov

Summary

The Integrated Renewable Energy System (IRES) testbed demonstration at the Pacific Northwest National Laboratory (PNNL) Sequim campus includes development of a suite of capabilities for tracking the performance of photovoltaic (PV) renewable energy components located on a floating platform (floating PV) and on a shoreline building rooftop. The marine environment represents potentially harsh and corrosive conditions for PV modules. Compared to terrestrial PV, potential concerns for offshore PV arising from high humidity and occasional contact with saltwater, marine wildlife, and aquaculture. These environmental factors can reduce electricity generation efficiency and increase the risk of electrical faults, polymer insulation or jacketing degradation and hydrolysis of the PV cell encapsulant materials. Offshore PV modules may also be exposed to lower temperatures and buoyant and vibrating motions with a floating platform. It is not clear how the long-term performance of floating PV will be affected by these factors. To understand expected energy generation through solar cells on a floating platform, monitoring of the performance of PV modules in the marine environment is needed. This report outlines a plan for long-term testing of IRES PV components utilizing resources of the PNNL Material Aging and Detection (MAaD) Science team and the Marine and Coastal Research Laboratory (MCRL). Equipment applicable for onsite testing and real-time monitoring of the PV performance associated with environmental conditions including temperature, solar irradiance, shading and soiling is included. In case of performance loss, equipment for fault detection, failure analysis, material testing, and further troubleshooting are also available. Through establishment of this capabilities, the enabling IRES project sets the stage for future research to advance off-shore and near-shore energy options for businesses and communities.

Acknowledgments

This work was performed at the Pacific Northwest National Laboratory in Richland, Washington and Sequim, Washington. Funded for the work was provided by the State of Washington. The Pacific Northwest National Laboratory is operated by Battelle for the U.S. Department of Energy under Contract DE-AC05-76RL01830.

Table of Contents

1. Background

Pacific Northwest National Laboratory (PNNL) operates the Department of Energy's (DOE) only dedicated marine laboratory at the PNNL-Sequim campus. PNNL is leading research in the blue economy and marine energy applications and building collaboration between DOE and multiple partners in the state of Washington and beyond. Established with Washington State support, the Integrated Renewable Energy System (IRES) demonstration testbed will advance research by developing and testing renewable energy production, management, and use for multiple marine applications (e.g., ocean observations, underwater vehicles, aquaculture). IRES will also advance energy resiliency for coastal communities by developing an integrated renewable energy test platform that will model how multiple renewable energy resources could power shoreline businesses or communities. The test bed will demonstrate how different renewable systems can be integrated to reduce carbon emissions and contribute to a net zero emissions site and provide lessons, controls, and protocols that will help to expand energy options for shoreline and maritime businesses. The integrated system is expected to serve as a test bed for shoreline power and ocean energy technologies for years to come.

One of the goals of the IRES project is to demonstrate use of renewable energy resources, including solar energy, as could be used to help power shoreline businesses or communities. The marine environment represents potentially harsh and corrosive conditions for photovoltaic (PV) modules. Compared to terrestrial PV, potential concerns for offshore PV arising from high humidity and occasional contact of saltwater include the increased risk of electrical faults, polymer insulation or jacketing degradation and hydrolysis of the ethylene-vinyl acetate (EVA) cell encapsulant. Offshore PV modules may also be exposed to lower temperatures, buoyant and vibrating motions with a floating platform, and a different ecosystem than onshore module. It is not clear how the long-term performance of floating PV will be affected by these factors.

To understand expected energy generation through solar cells on a floating platform, monitoring of the performance of PV modules in the marine environment is needed. This report outlines a plan for long-term testing utilizing resources of the Pacific Northwest National Laboratory (PNNL) Material Aging and Detection (MAaD) Science team and the Marine and Coastal Research Laboratory (MCRL). Table 1 lists equipment applicable for onsite testing and real-time monitoring of the PV performance associated with environmental conditions including temperature, solar irradiance, shading and soiling. In case of performance loss, equipment for fault detection, failure analysis, material testing, and further troubleshooting are also available. Details about the equipment are discussed in Section 2.

Table 1. Equipment used for long-term monitoring of PV performance.

Equipment	Properties measured	Functions
PV performance analyzer	Current, Voltage, Power	PV performance assessment, detection and troubleshooting of performance loss, screening
Electroluminescence imaging	Photos of the module; dark region indicates an anomaly	Detection of visually invisible anomalies (e.g., cracking)
Infrared thermography	Thermographs of the module and balance of system; hot region indicates an anomaly	Detection of "hot spots" (e.g., short circuit), monitoring unfavored environmental factors (e.g., soiling)
Spectrometers	Molecular structures	Material identification, degradation of polymer encapsulant and backsheet

Temperature and irradiance sensors	Cell temperature, direct and reflected irradiance, albedo, soiling	Monitoring of solar energy and expected power output
Spread spectrum time domain reflectometry (SSTDR)	Pseudo-noise voltage wave signal reflections	Location of faults in circuit

The data obtained from the PV monitoring task will be an asset to offshore PV-related research and applications and will be shared with the community. Examples of further analysis of data include estimation of the levelized cost of electricity (LCOE) of a floating PV system. PV data can be integrated into existing Department of Energy (DOE) sponsored datahubs, such as the MCRLdata mcrldata.pnnl.gov, the DuraMAT data hub datahub.duramat.org, and the PV Performance Modeling Collaborative (PVPMC) datasets pvpmc.sandia.gov/datasets.

In addition to filling a data gap, the experience of testing offshore PV modules from a remote location is helpful for developing a standard procedure for floating PV testing that is not currently available. Challenges identified for long-term PV stability in a marine environment can also inform researchers and manufacturers of the needs for the next-generation PV devices, for example, to improve the moisture resistance.

2. Equipment

Portable equipment and sensors were purchased to test performance of a floating PV system in the service and to compare with performance between PV panels on a floating platform with those on a terrestrial rooftop. This section elaborates the basic principles of equipment, the properties being tested, and how the equipment can help reveal anomalies in PV devices.

2.1 PV Modules and Inverter

Crystal silicon (Si) is the most common semiconductor used in solar cells, representing approximately 95% of the PV market in 2022 [1,2]. Cadmium telluride (CdTe) is the second most common material and constitutes around 5% of the solar panels in the world market. Other materials used to make solar cells are listed in Table 2 with quantum efficiency values of research cells and lifetime stability information from the literature listed for reference.

Table 2. Commonly used semiconductor materials for single-junction PV cells [1,3].

Semiconductor Materials		Advantages and Limitations
Silicon (Si)	Monocrystalline	• Low cost • High efficiency: up to 27.6% [2], approaching the single-junction theoretical limit of 29.4% [1]. • Long lifetime: >25 years in harsh outdoor environment with <0.5% annual degradation [1].
	Polycrystalline	
	Amorphous	
Thin film	Cadmium telluride (CdTe)	• Cost-effective: due to less material usage and lower requirement in material purity • Lower efficiencies than Si: up to 22.4% [2] • Suitable for building-integrated PV including as semi-transparent windows [4]
	Copper indium gallium diselenide (CIGS)	• High efficiency in the lab: up to 23.6% [2] • Not scaled up yet due to the challenge in combining four elements to fabricate a large module
Emerging technologies	Perovskite	• High efficiency in the lab: 33.9% for perovskite/Si tandem [2] • Not stable in outdoor environment
	Organic	• Low efficiency • Short lifetime
	Quantum dots	

Crystalline Si panels were chosen for study due to their predominancy in the market. The crystalline Si module technology has been developing rapidly for increased power output and cell efficiency [1,5]. The passivated emitter and rear contact (PERC) cells dominate the market in 2021 as shown in Figure 1. The massive production of PERC since 2016 has also driven down the production cost of bifacial modules [6] and increased the adoption of bifacial solar technology by commercial and utility-scale solar developers. The bifacial modules can collect photons from incident and albedo light from front and rear sides, which enhances the power producing capability per area and reduces the land use [7]. Bifacial gain measures the increase in the energy yield by a bifacial module compared to that by a monofacial module with similar groundcovers (background reflections). The bifacial gain against a white and natural groundcover is in the range of 8-18% and 2-11% respectively [6].

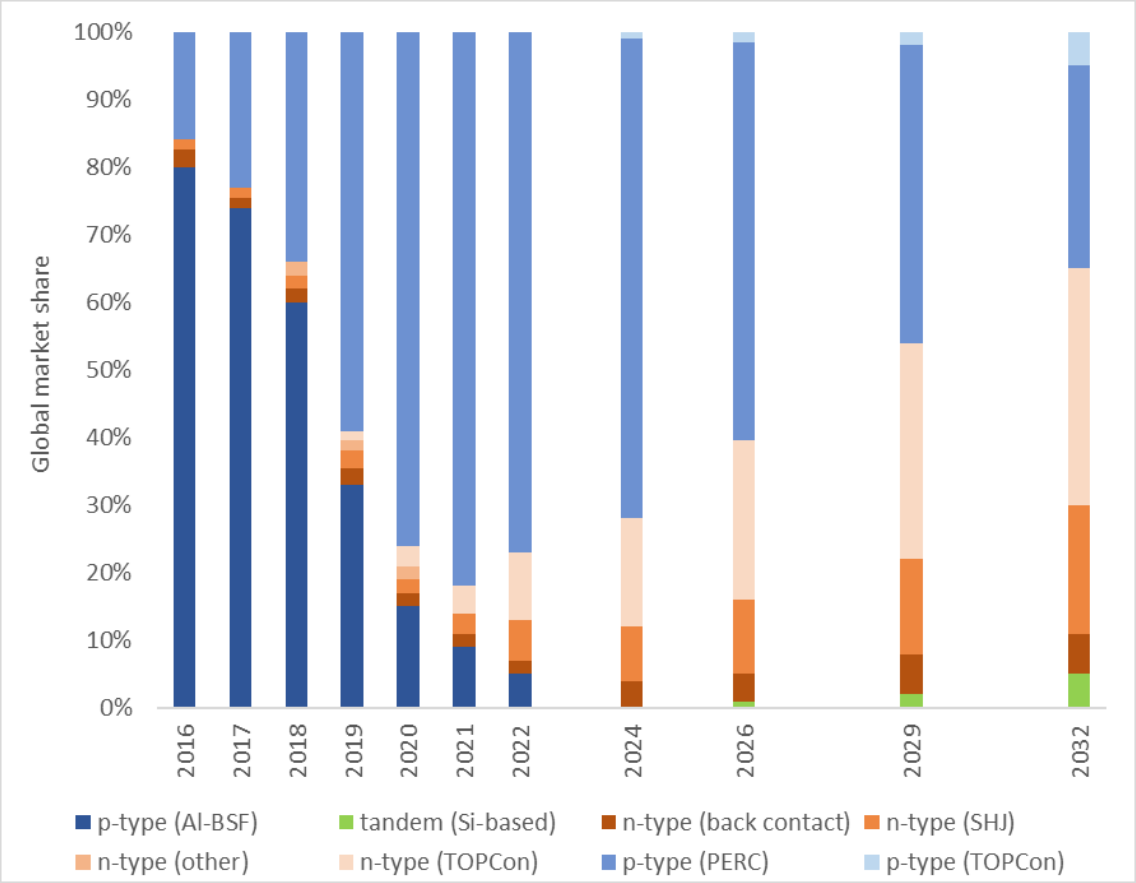

Figure 1. Historical (2016 – 2021) and projected (2022 – 2032) market share of crystal Si cell technologies. Al-BSF: aluminum-back surface field, SHJ: silicon heterojunction, TOPCon: tunnel oxide passivating contact, PERC: passivated emitter and rear contact. Adapted from a presentation on 2023 PV reliability workshop [5].

Monofacial and bifacial modules were purchased from Q CELLS for the IRES project to be installed on the floating platform. The specifications are given in Table 3.

Table 3. Specifications of Q CELLS PV modules

	Monofacial	Bifacial
Model	Q.PEAK DUO XL-G10.2 480	Q.PEAK DUO XL-G10.3 / BFG 480
Format	87.2 in × 41.1 in × 1.38 in	87.2 in × 41.1 in × 1.38 in
Front cover	Glass	Glass
Back cover	Composite film	Glass
Frame	Anodized aluminum	Anodized aluminum
Efficiency, η (%)	≥20.7 at STC*	≥20.7 at STC*, ≥22.7 at BSTC†
Maximum power, P_{max} (W)	480 at STC*	480 at STC*, 525 at BSTC†
Current at MPP‡, I_{mp} (A)	10.71 at STC*	10.59 at STC*, 11.58 at BSTC†
Voltage at MPP‡, V_{mp} (V)	44.81 at STC*	45.33 at STC*, 45.32 at BSTC†
Short circuit current, I_{sc} (A)	11.26 at STC*	11.12 at STC*, 12.17 at BSTC†
Open circuit voltage, V_{oc} (V)	53.61 at STC*	53.39 at STC*, 53.58 at BSTC†
*STC: standard test conditions: solar irradiance 1000 W/m^2, cell temperature 25±2 °C, air mass 1.5 †BSTC: bifacial standard test conditions: front irradiance 1000 W/m^2, rear irradiance 135 W/m^2, cell temperature 25±2 °C, air mass 1.5 ‡MPP: maximum power point		

Along with the PV modules, a solar inverter (SMA, Sunny Tripower X 20-US, STP 20-US-50) is used to convert the direct current (DC) output from the modules into an alternating current (AC) that can be used by appliances or fed into the electrical grid.

2.2 Electrical Output Performance

2.2.1 Portable Current-Voltage (I-V) Curve Tracer

The I-V characteristics of PV devices can be measured on strings, modules, and arrays of devices. A typical I-V curve is given in Figure 2, which ranges from the short circuit current (I_{sc}) at 0 voltage to the open circuit voltage (V_{oc}) at 0 current. A key parameter is the maximum power (P_{max}) which manifests as a knee on the I-V curve. The voltage and current at P_{max} are V_{mp} and I_{mp} respectively.

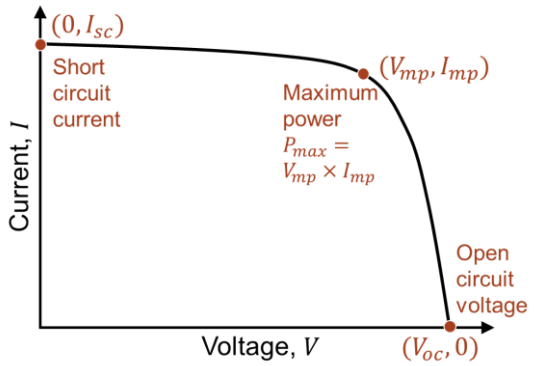

Figure 2. Illustration of a characteristic I-V curve of a PV device showing three points.

I-V performance of a PV device can be affected by solar irradiance, temperature, other environmental factors such as shading, panel orientation, and the health of the test device. Standard test conditions (STC) are specified in the 60904 series of International Electrotechnical Commission (IEC) standards, being 1000 W/m^2, 25 °C, with the IEC 60904-3 reference solar spectral irradiance distribution AM1.5G. Manufacturers typically provide the I-V parameters at STC, for example, as shown in Table 3, for the monofacial and bifacial Q CELLS modules. At other temperature (T) and irradiance (G) conditions, I-V curves will have the same shape as the curve in Figure 2 but will exhibit different voltage and current values. The I-V curve at a random condition (T_2, G_2 in Figure 3) can be scaled to a target condition (T_1, G_1 in Figure 3) such as the STC following IEC 60891, “Photovoltaic devices - Procedures for temperature and irradiance corrections to measured I-V characteristics”, where empirical equations describing the temperature and irradiance dependences of voltage and current are used to map every point on the I-V curve, as shown in Figure 3. The empirical equations can be found in IEC 60891 as well as in a Sandia report “Photovoltaic Array Performance Model” [8]. A rule of thumb is that current increases with irradiance and voltage increases with temperature. A web based I-V curve correction tool has been launched by Berkeley lab: https://pvtools.lbl.gov/iv-curve-correction-tool.

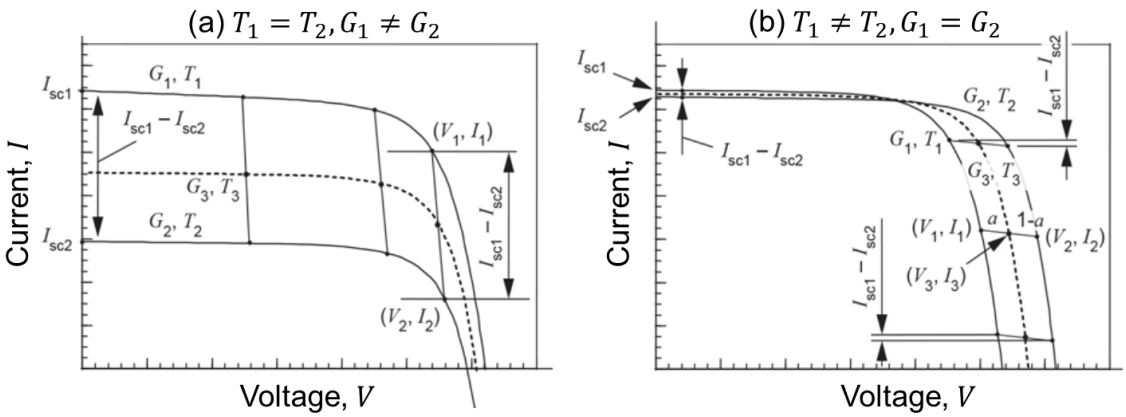

Figure 3. Examples of (a) irradiance correction and (b) temperature correction of I-V curves. Adapted from IEC 60891 [9].

The shape of I-V curve can help troubleshoot potential performance issues of tested PV devices. For example, as shown in Figure 4, the notches and steps on the I-V curve can be attributed to partial shading of the PV string. The notches indicate a reduction in current capacity, which could also be caused by damage of the PV cell. Cracking of the cell would have the same effect on the I-V curve as shading of an equivalent area.

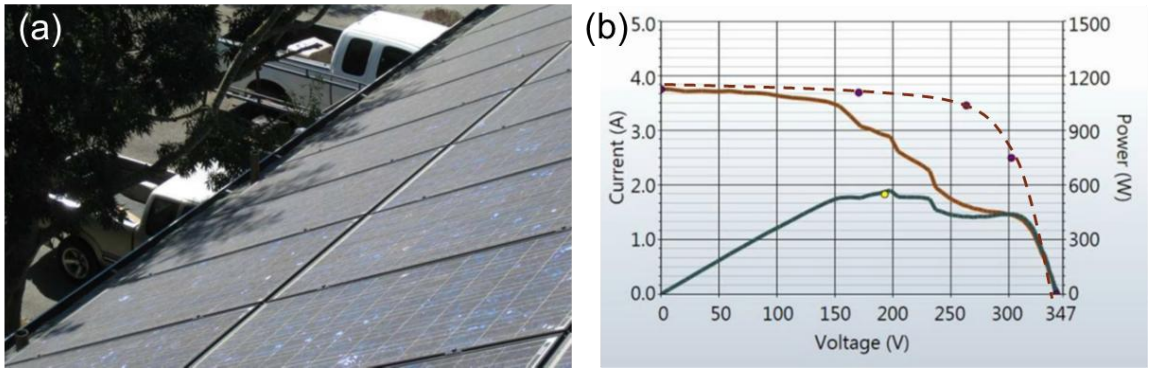

Figure 4. An example of (b) notches or steps on the I-V curve (red solid) caused by (a) partial shading the PV string under test. Green solid: power-voltage curve. Red dashed: a theoretical I-V curve of the string without shading [10].

If the shape of I-V curve is not affected, other parameters including I_{sc}, V_{oc} and P_{max} should be recorded and compared to manufacturer specifications or historical data. Module degradation can result in higher resistance and drops in I_{sc} and P_{max}.

For long-term monitoring of PV within the IRES project, a portable I-V tracer (Solmetric PVA-1500HE-30AMP) was purchased along with a reference sensor (Solmetric SolSensor 300) to read irradiance, module temperature and tilt angle. A shade measurement tool (Solmetric SunEye-210) is used to evaluate the solar access of the site over time. A sample I-V curve as shown in Figure 5 was obtained for a small research cell graciously provided by the Solar Durability and Lifetime Extension (SDLE) Center at Case Western Reserve University.

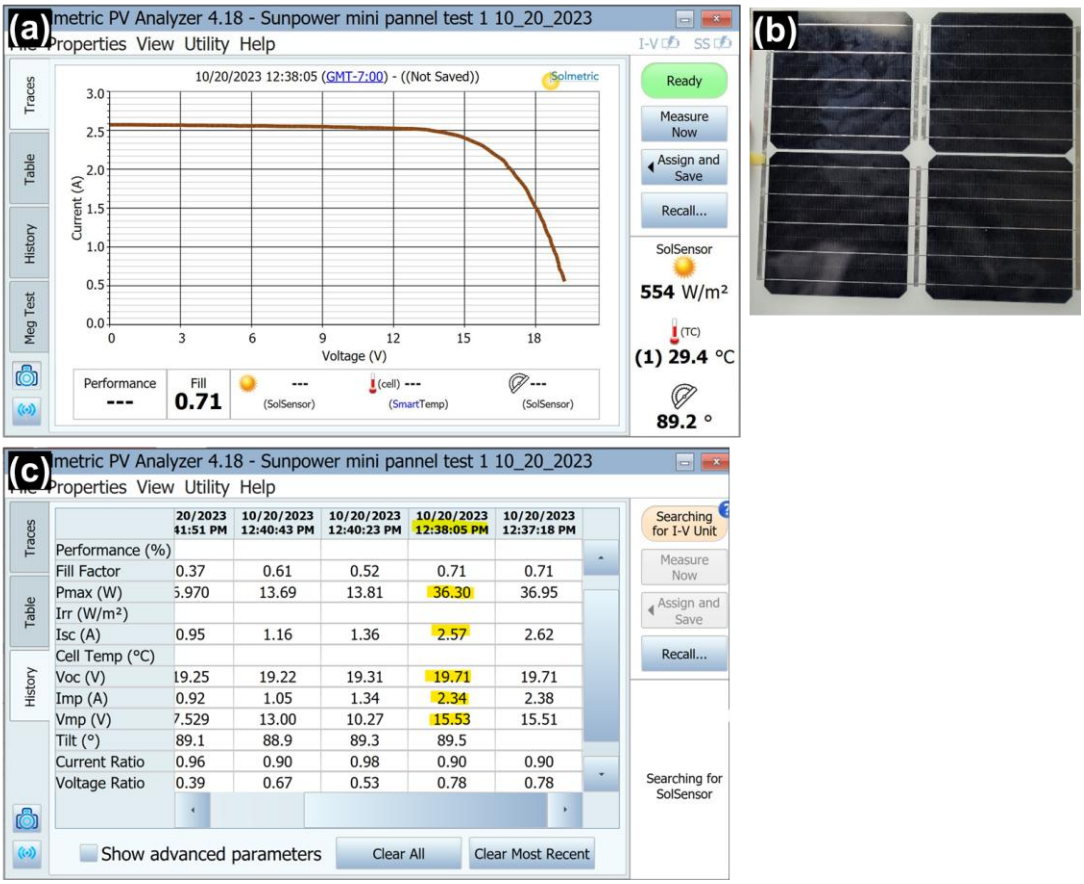

Figure 5. Screenshots of the PV analyzer showing (a) the I-V curve, (c) the characteristic parameters of (b) a small-size research cell.

2.3 Failure Detection and Analysis

2.3.1 Portable Electroluminescence (EL) Imaging System

Electroluminescence (EL) is the phenomenon in which a material emits radiation in response to the passage of an electric current or to a strong electric field. The EL emission spectra of the most used semiconductor materials for PV cells are given in Figure 6 [11]. Their peak wavelengths are labeled in Figure 6 and fall in the near-infrared (near-IR) spectral range (780 nm to 2500 nm). Other PV materials also have EL emission spectra in near-IR range. For example, the emission spectrum of amorphous Si is broader than crystalline Si and peaks at around 1200 nm [12]. The emission peak of organic PV resides at longer wavelengths (1200 nm – 1400 nm) [12].

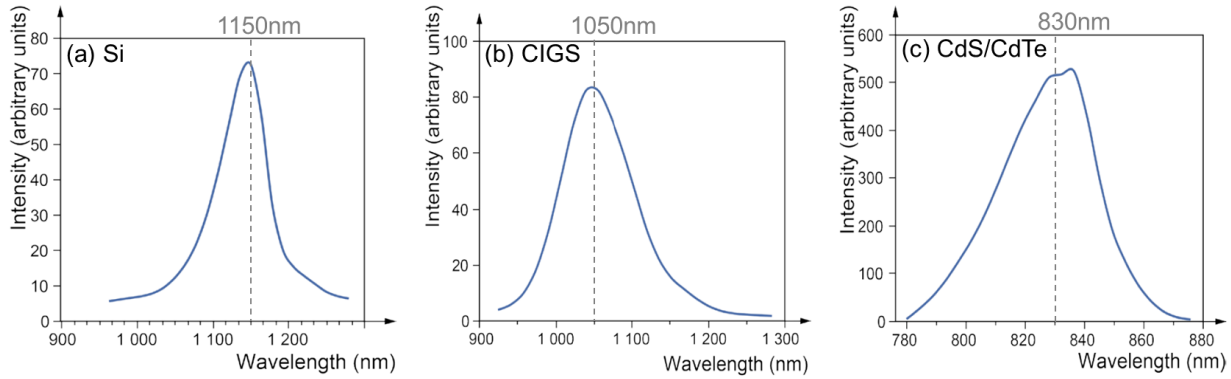

Figure 6. EL emission spectra for (a) crystalline Si, (b) copper indium gallium diselenide (CIGS), ZnO/CdS/Cu(In,Ga)Se_2, and (c) cadmium sulfide/cadmium telluride (CdS/CdTe) heterostructure solar cells. Adapted from IEC TS 60904-13 [11].

The EL imaging system can capture the EL emission of PV modules that is invisible to the human eye. It is a non-destructive technique to distinguish between failure modes. Defects can be detected using the EL camera and attributed to degradation during different stages of the PV module lifetime, from production to transportation, installation, and application. While reduced performance based on location within a panel may be easily obtained and tracked by EL, attribution of reduced performance to specific failure modes based on the patterns and signal intensities of EL photos may require advanced material knowledge and expertise. In the Annex D of IEC TS 60904-13:2018 “Photovoltaic devices – Part 13: Electroluminescence of photovoltaic modules”, sample EL images can be found for crystalline Si PV modules with typical defects and interpretations of probable causes. Three examples are taken from IEC TS 60904-13 and shown in Figure 7.

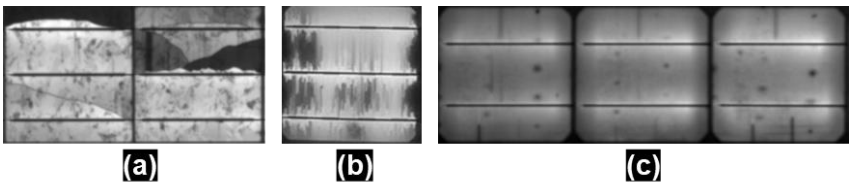

Figure 7. EL images of crystalline Si modules with defects, including (a) cell cracking, (b) missing or broken grid fingers, and (c) localized shunting caused by material contamination. Adapted from IEC TS 60904-13 [11].

For the PV monitoring task on this project, the EL imaging system (TravEL-Spot, BrightSpot Automation, LLC) can be profitably applied to inspection of PV modules at all stages during PV array construction, including but not limited to upon receipt the new panels in Richland, WA, following transported to Sequim, WA, following installation on the floating platform, and after the IRES starts to generate electricity. The EL system at PNNL contains the following key components: (1) an EL camera (Nikon Z 6) with filters to block wavelengths outside the emission spectra of solar cells, (2) a power supply (BK Precision 1902B) to provide sufficient voltage to achieve short-circuit current (I_{sc}), and (3) the software (IMPEL) for power supply control, image acquisition and post-processing. Baseline testing of two new PV panels have been conducted in the lab, with the setup demonstrated in Figure 8(a). A sample photo is shown in Figure 9, indicating no obvious defects. The EL imaging system can also be used outdoor with optional setups shown in Figure 8(b)(c).

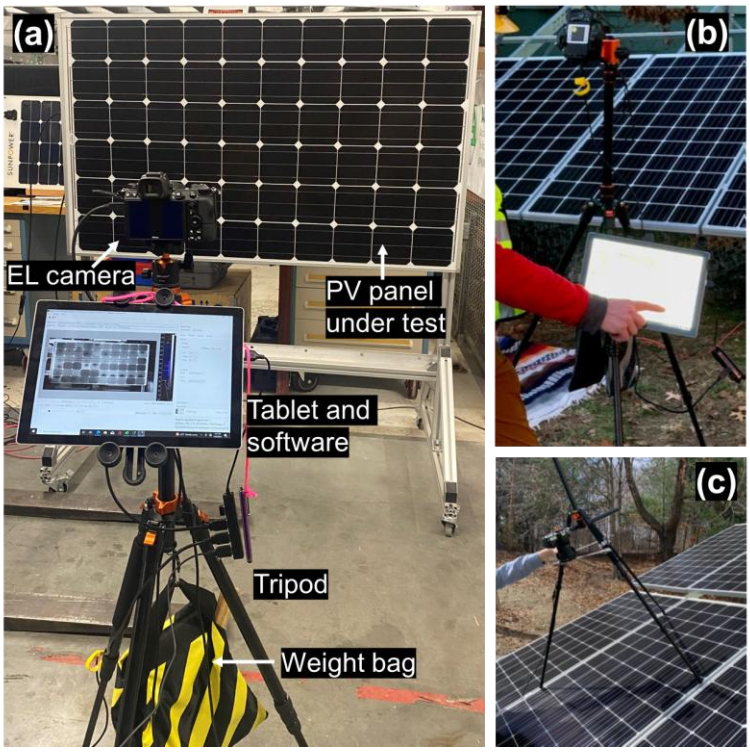

Figure 8. Setups for EL imaging (a) in a PNNL lab, and (b)(c) in the field (adapted from www.brightspotautomation.com)

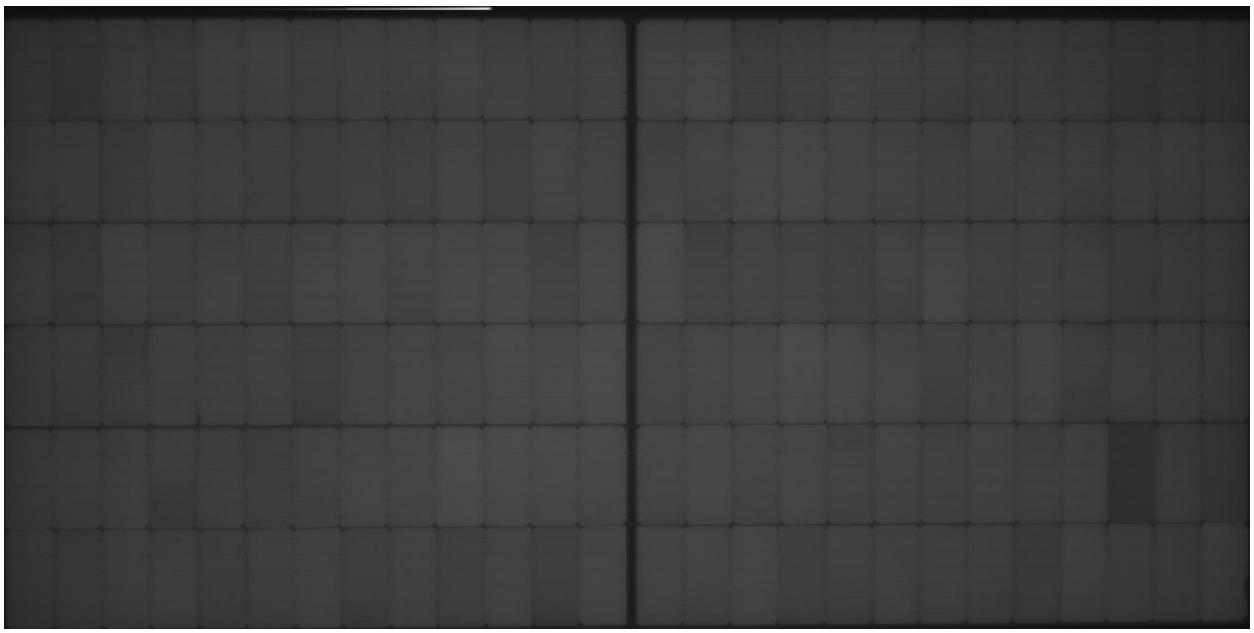
Figure 9. An EL photo obtained for a Qcell PV panel using TravEL-Spot EL imaging system under its open circuit voltage (50 V) at room temperature (20 °C) inside the lab at 2410STV building at PNNL (Richland, WA).

2.3.2 Portable Infrared (IR) Thermography

IR thermography uses an infrared camera to capture images of emitted black-body radiation from the objects. For an ideal black body in thermodynamic equilibrium, the emitted radiation is

a continuous spectrum that depends on its temperature according to Planck's law as in Equation (1).

$$B_\nu = \frac{2h\nu^3}{c^2}\frac{1}{\exp(h\nu/kT) - 1} \tag{1}$$

where B_ν = spectral radiance
ν = frequency
T = absolute temperature
h = Planck constant
c = speed of light in vacuum
k = Boltzmann constant

At higher a temperature, the spectral radiances (B_ν) at a given frequency increases and the peak shifts to a shorter wavelength. However, very few objects are true black bodies. For a real surface, the radiant emittance (M_e, being the radiant flux emitted per unit area) is smaller than that of a black body radiator (M_e°), with the ratio being the emissivity (ε), as given by Equation (2).

$$\varepsilon = \frac{M_e}{M_e^\circ} \tag{2}$$

The correlation between B_ν and M_e° are given by Equation (3) where [=] means the characteristic units of both sides are the same.

$$\pi B_\nu [=] M_{e,\nu}^\circ = \frac{\partial M_e^\circ}{\partial \nu} \tag{3}$$

Emissivity depends on materials, varying between 0 and 1. High emissivity materials ($\varepsilon > 0.95$) include uncoated glass, pure water, ice, human skin. Polished pure copper has very low emissivity ($\varepsilon = 0.04$) while the oxidized copper has a high emissivity ($\varepsilon = 0.87$). Air has near-zero emissivity. The IR camera measures radiant emittance (M_e) based on which the connected software calculates temperatures with an input emissivity parameter. If the emissivity input for the target material is not correct, the temperature given by the software will also be incorrect.

IR imaging enables seeing human bodies and warm-blooded animals through visual obstacles such as smokes and dim lights. The technology has been widely used in many fields such as fireground search, clinical diagnostics, surveillance cameras. IEC TS 62446-3:2017, "Photovoltaic (PV) systems – Requirements for testing, documentation and maintenance – Part 3: Photovoltaic modules and plants – Outdoor infrared thermography", gives detailed instructions on a thermographic inspection of PV modules and balance-of-system (BOS) components of PV power plants. Examples of BOS components are cables, fuses, inverters, and switchgears [13]. An example of an identified hot spot inside a PV string combiner box is

shown in the red-boxed areas in Figure 10.

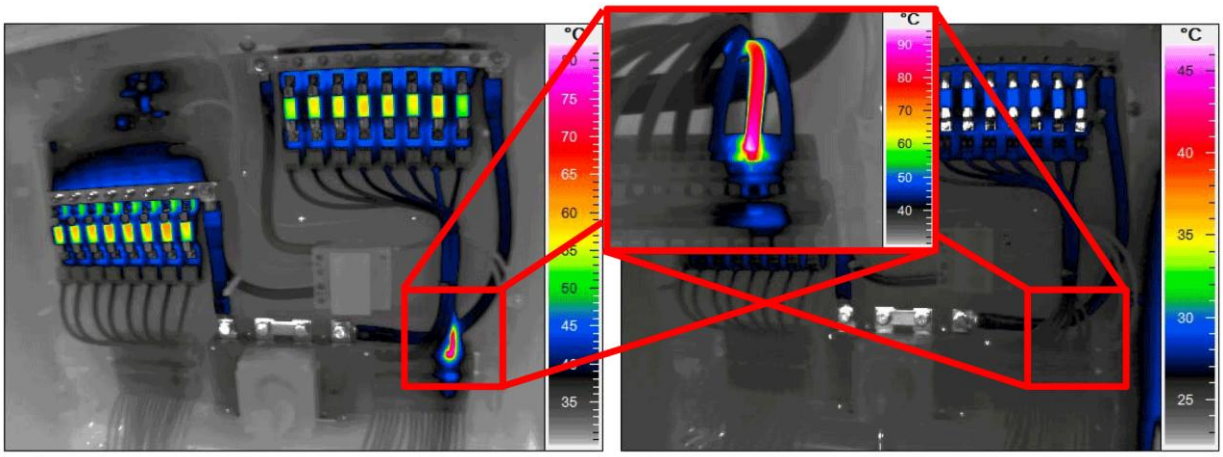

Figure 10. The IR thermograms of a PV string combiner box before (left) and after (right) maintenance on a faulty contact (red-boxed). Adapted from IEC TS 62446-3:2017 [13].

Inspections on PV modules using IR thermography are suggested to be performed at high solar irradiance ($> 600\,W/m^2$) and constant ambient conditions (no clouds, low wind speed, stable ambient temperature), with the PV modules energized and the PV power plants in operation. Operational conditions are required for two reasons: (1) If there is an inactive module or string, the solar energy will not be converted to electricity and will be emitted as heat, which will be detected using IR camera as a “hot spot”. High solar irradiance is required to increase the contrast between functioning (cool) and inactive (hot) regions on the PV modules. (2) While IR images can reflect problems internal to PV modules such as open circuit, short circuit, broken front glass, etc., external conditions such as cloud, wind, shading, and soiling can also result in non-uniform temperatures throughout the module surface. The external factors must be kept constant and the module clean to reveal potential internal problems. Figure 11 shows the example of how dirt on cells can manifest as abnormalities on the IR thermograph. The temperature in the hot spot in Figure 11 was also skewed due to the difference in emissivity between glass and dirt.

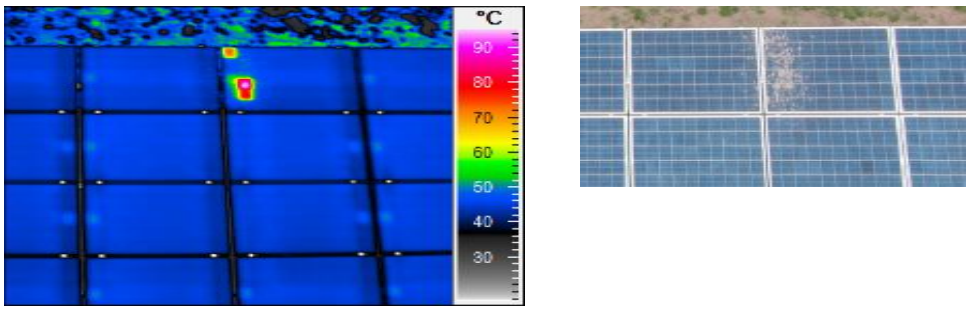

Figure 11. Hot spot of a PV module (left) due to cells shaded by dirt (right). Adapted from IEC TS 62446-3:2017 [13].

A portable IR thermography system (Teledyne FLIR A700 Professional Science Kit) was purchased for periodic inspection of PV modules on the floating platform, as shown in Figure 12. The system includes a thermal camera with 640 x 480 resolution, 7.5 µm to 14 µm wavelength range, and -20 °C to +120 °C object temperature range, which fulfills the requirements for inspecting PV plants as specified by IEC TS 62446-3:2017. A live stream view of the IR camera can be seen from the controlling software (FLIR Research Studio). The software also allows

enter material parameters such as emissivity and reflected temperature. The system is ready for use when weather permits, especially when solar irradiance is above $600\,W/m^2$.

Figure 12. Portable IR thermography equipment

2.4 Polymer Degradation Detection

Polymers are used as PV panel backsheets and encapsulants to protect the active layers against unfavored weathers, mechanical influences during handling and transportation, and to ensure electrical insulation. Degradation of polymers can affect the reliability and service life of a PV module. Detection and monitoring of polymer aging is a task in many fields and is often assisted by spectroscopic methods, including Fourier-transform infrared (FTIR), Raman, ultraviolet-visible (UV-vis), and visible color change, covering a wavelength range from nm to cm, as shown in Figure 13. In this range the mid-IR (MIR) region is the most useful for detection of organic polymers and inorganic silicon and glasses.

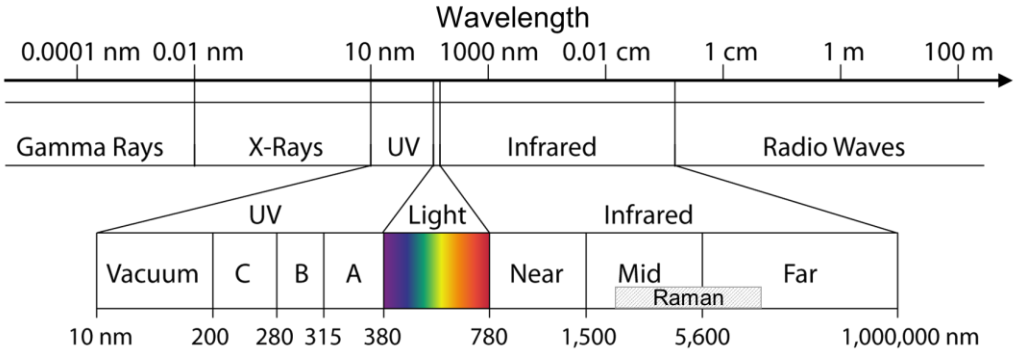

Figure 13. The wavelength range of UV, visible, and IR regions in an electromagnetic spectrum.

FTIR and Raman spectroscopy are complementary to identify materials based on the location of characteristic absorption peaks of molecular structures (such as C-C, C-H, etc.). The differences between these two techniques include (1) that FTIR measures the energies of photons not absorbed while Raman measured the energies of scattered photons, and (2) that FTIR is more sensitive to asymmetric vibrations of polar groups whereas Raman can better resolve symmetric vibrations of non-polar groups.

UV-vis spectrometry and colorimetry are useful for detection of polymer degradation products, especially when double bonds (C=C, C=O) are formed. Since the polymer layers are typically

transparent or near-white, formation of the conjugated structures can often be visually observed as yellowing.

To facilitate non-destructive, on-site testing, handheld tools were purchased, as listed in Table 4.

Table 4. Handheld equipment for polymer degradation monitoring.

Equipment	Make	Model	Functions
Handheld FTIR spectrometer	Agilent Technologies	4300 HH FTIR	Material identification, polymer oxidation and degradation tracking
Handheld Raman spectrometer	Agilent Technologies	Resolve	Material identification
Handheld colorimeter	HunterLab	MiniScan EZ	Polymer degradation tracking

2.5 Online Monitoring

2.5.1 Temperature and Irradiance Sensors

Real-time monitoring systems of PV performance is commercially available for rooftop modules, which typically report power generation over different time periods, along with solar irradiance and temperature. The data can be accessed through web pages, computer software and phone apps. A similar monitoring system for floating PV will be beneficial to detecting anomalies, recording operating performance, and understanding longevity. Sensors listed in Table 5 will be used for data acquisition on IRES PV modules to build such a PV monitoring system.

Table 5. Sensors for real-time online monitoring of PV modules.

Sensor	Make	Model	Functions
Temperature sensor	Campbell Scientific	CS241DM-NC-PT	To measure back-of-module temperature
Pyrheliometer	Kipp & Zonen	SHP1-V	To measure the direct normal incidence (DNI) of solar radiation, within 5° view angle
Sun tracker	Kipp & Zonen	SOLYS2	To mount pyrheliometer
Pyranometer	Kipp & Zonen	SMP12	To measure the global (direct and diffused) solar radiation on a planar surface. A shaded pyranometer measures diffuse solar radiation.
Albedometer	Kipp & Zonen	CMF1 (mounting fixture)	To measure albedo (the ratio of the diffusely reflected and the total solar radiation) with two pyranometers one facing up and one facing down
Soiling monitor	Kipp & Zonen	DustIQ	To measure transmission light with photodiode and calculate soiling ratio based on the loss of transmission

2.5.2 Spread Spectrum Time Domain Reflectometry (SSTDR)

Spread spectrum time domain reflectometry (SSTDR) technology is used to monitor live circuits and to locate faults (such as opens and shorts). As shown in Figure 14, a PV panel is connected to the waveform generator (Siglent, SDG7102A) and the oscilloscope (Pico Technology, 6462E) via an inline fault trapper. A voltage wave is sent to the PV panel. If an impedance change is encountered due to an anomaly, part of the energy is reflected and captured by the oscilloscope. The time delay between wave initiation and reflection detection, combined with the wave propagation velocity, can reveal the distance between the fault and the waveform generator. SSTDR has been applied to low voltage energized systems including live PV arrays

to find the position of faults [14]. The fault detection system for PV testing was adapted from previous cable condition monitoring research in the Acceleration and Realtime Environmental Nodal Assessment (ARENA) testbed at PNNL (www.pnnl.gov/arena/).

Figure 14. Overview of SSTDR setup at PNNL

3. Plan for PV Performance Testing

3.1 Onsite Long-term Testing

As mentioned, it is unknown how the marine environment (high humidity, low temperature, movement with the base platform, and ecosystem) can affect the performance and degradation of commercial PV modules. A long-term test is suggested in Sequim Bay for PV modules installed on IRES floating platform. In parallel, a control PV module is needed for comparison. The location of the control module needs to be near the bay and on the land to experience similar solar irradiation. Figure 15 is an example of potential locations for the offshore and terrestrial PVs near PNNL Sequim facility.

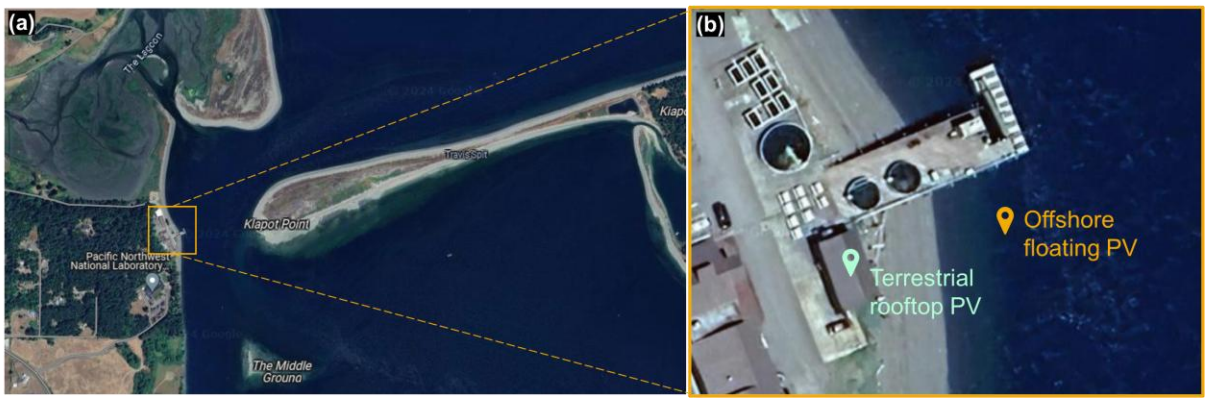

Figure 15. Potential locations for offshore and terrestrial PV modules to be monitored.

Monofacial and bifacial crystal-Si modules were purchased as discussed in Section 2.1 to estimate the bifacial gain at the marine environment and its impact on electricity generation. Other types of modules, such as those made with CdTe, or with a different architecture (Figure 1), are worth investigating, as the material system and device architecture may be affected by marine environments differently.

A potential timeline for periodic inspection of installed PV modules is proposed in Figure 16. A thorough check of the delivered modules is recommended to make sure that the performance is consistent with manufacturer specifications, and that no damage was caused during transportation. I-V curves and EL images would be particularly informative for initial checking of as-received modules. Care should be taken during installation to avoid damage to the panel cells. It is worthwhile to go through all the tests again immediately following installation to establish a baseline and to detect any damage induced by handling.

Figure 16. Potential timeline for monitoring and periodic inspection of PV modules. "As-received": purchased PV modules delivered to PNNL-Sequim but not installed. "0 years": right after installation

Following installation, the sensors listed in Table 5 (Section 2.5.1) would stream data to the controlling software to help determine if there is any rapid drop in performance ratio, in which case the equipment described in Section 2 combined with information gathered through the environmental monitoring system (e.g., wind speed, wave height, and underwater event) will help troubleshoot the PV performance issue. Periodic tests at the intervals proposed in Figure 16 or more frequently are suggested to identify PV failure and to understand the performance loss rate (PLR) and materials degradation rate in marine environment.

3.2 In-lab Testing of Accelerated Degraded Modules

To assist management of a floating PV facility, a model is needed to estimate the PLR especially those irrecoverable, degradation-induced PLR. Models for offshore PV must consider the effects of humidity and salt concentration, which are either lacking [15] or convoluted with temperature and irradiance [16,17] in current models. In parallel to the long-term onsite monitoring, testing of small-size modules exposed to accelerated degradation conditions in a weathering box can provide data for developing lifetime prediction models.

Accelerated aging tests have been used for design qualification and type approval of terrestrial PV modules in open-air climates, as specified in IEC 60721 for Si modules and IEC 61646 for thin-film modules. Although there is not yet a complete guide on accelerated aging tests for floating PV, established tests as listed in Table 6 can be performed to guide the path forward.

Table 6. Potential tests under accelerated degradation conditions [18]

Test	Factors	Degradation mechanism / failure mode
Damp heat	High temperature, high humidity	Corrosion, encapsulant adhesion, junction box adhesion, delamination
Humidity freeze (frosting)	Low temperature, high humidity	Junction box adhesion, delamination, inadequate edge deletion
Salt mist spray	Salt concentration, high humidity	Corrosion

4. Conclusion

The IRES testbed demonstration project at PNNL integrates energy production, storage, management, and use components for multiple marine energy applications. Offshore solar generation is a relatively untapped source of electrical energy that could meaningfully contribute to offshore applications as well as the energy needs of coastline businesses and communities. The harsh environmental conditions expected to be experienced by floating photovoltaic equipment including encounters with seawater, marine life, aquaculture, and tidal motion may severely affect PV performance and lifetime.

This PV monitoring task of the IRES project identified technologies for tracking and troubleshooting PV performance. Establishment of a suite of capabilities for PV module monitoring encompassed procurement of portable and laboratory test equipment, demonstration of equipment testing on commercial PV modules, and generation of a proposed long term testing plan. Assembled test capabilities include measurement of generated current, voltage, and power for assessment of performance efficiency. Electroluminescence imaging reveals spatial anomalies such as do to cracking. Hot spots visible from Infrared thermography show short circuits and environmental factors such as soiling. Spectrometers identify material degradation of PV back sheets and encapsulant layers. Temperature and irradiance sensors correlate environment with expected output, and online spread spectrum reflectometry can reveal intermittent faults during operation.

A plan for tracking and predicting long term floating PV module performance was established including ongoing monitoring of deployed systems at PNNL-Sequim and accelerated aging and testing of PV modules at PNNL-Richland. It is anticipated that the capabilities in PV monitoring established through the IRES project will help to unlock the energy resource of floating PV in future research.

5. References

[1] P. Verlinden, D.L. Young, G. Xiong, M.O. Reese, L.M. Mansfield, M. Powalla, S. Paetel, R.M. France, P.T. Chiu, N.M. Haegel, Photovoltaic device innovation for a solar future, Device. 1 (2023) 100013. https://doi.org/https://doi.org/10.1016/j.device.2023.100013.

[2] National Renewable Energy Laboratory, Best Research-Cell Efficiency Chart, (n.d.). https://www.nrel.gov/pv/cell-efficiency.html (accessed February 20, 2024).

[3] Solar Energy Technologies Office, Solar Photovoltaic Cell Basics, (n.d.). https://www.energy.gov/eere/solar/solar-photovoltaic-cell-basics (accessed February 20, 2024).

[4] M.J. Sorgato, K. Schneider, R. Rüther, Technical and economic evaluation of thin-film CdTe building-integrated photovoltaics (BIPV) replacing façade and rooftop materials in office buildings in a warm and sunny climate, Renew. Energy. 118 (2018) 84–98. https://doi.org/https://doi.org/10.1016/j.renene.2017.10.091.

[5] J. Zuboy, M. Springer, E. Palmiotti, J. Karas, B. Smith, M. Woodhouse, T. Barnes, DuraMAT Technology Scouting Report: Assessing Module Reliability Risks Associated with Projected Technological Changes, in: United States, 2023. https://www.osti.gov/biblio/1961564.

[6] K. Gibson, T. Erion-Lorico, Bifacial PV Module Energy Modeling Validation Study, United States, 2023. https://doi.org/10.2172/2229719.

[7] G. Raina, S. Sinha, A simulation study to evaluate and compare monofacial Vs bifacial PERC PV cells and the effect of albedo on bifacial performance, Mater. Today Proc. 46 (2021) 5242–5247. https://doi.org/https://doi.org/10.1016/j.matpr.2020.08.632.

[8] J.A. Kratochvil, W.E. Boyson, D.L. King, Photovoltaic array performance model., United States, 2004. https://doi.org/10.2172/919131.

[9] International Electrotechnical Commission, Procedures for temperature and irradiance corrections to measured I-V characteristics, IEC. 60891 (2021).

[10] Solmetric Corporation, Solmetric PV Analyzer™ I-V Curve Tracer User's Guide, 2022.

[11] International Electrotechnical Commission, Photovoltaic Devices-Part 13: Electroluminescence of photovoltaic modules, IEC TS. 60904–13 (2018).

[12] U. Jahn, M. Herz, D. Parlevliet, M. Paggi, I. Tsanakas, J. Stein, K. Berger, S. Ranta, R. French, M. Richter, Review on infrared and electroluminescence imaging for PV field applications, 2018. https://iea-pvps.org/wp-content/uploads/2020/01/Review_on_IR_and_EL_Imaging_for_PV_Field_Applications_by_Task_13.pdf.

[13] International Electrotechnical Commission, Photovoltaic (PV) systems - Requirements for testing, documentation and maintenance - Part 3: Photovoltaic modules and plants - Outdoor infrared thermography, IEC TS. 62446–3 (2017).

[14] S. Kingston, E. Benoit, A.S. Edun, F. Elyasichamazkoti, D. E. Sweeney, J.B. Harley, P.K. Kuhn, C.M. Furse, A SSTDR methodology, implementations, and challenges, Sensors. 21 (2021) 5268.

[15] J. Stein, PV Performance Modeling Methods and Practices: Results from the 4th PV Performance Modeling Collaborative Workshop., United States, 2017. https://doi.org/10.2172/1347082.

[16] C.-C. Lin, Y. Lyu, D.S. Jacobs, J.H. Kim, K.-T. Wan, D.L. Hunston, X. Gu, A novel test method for quantifying cracking propensity of photovoltaic backsheets after ultraviolet exposure, Prog. Photovoltaics Res. Appl. 27 (2019) 44–54. https://doi.org/https://doi.org/10.1002/pip.3038.

[17] D.E. Mansour, C. Barretta, L. Pitta Bauermann, G. Oreski, A. Schueler, D. Philipp, P. Gebhardt, Effect of backsheet properties on PV encapsulant degradation during combined accelerated aging tests, Sustainability. 12 (2020) 5208.

[18] K.-A. Weiß, E. Klimm, I. Kaaya, Accelerated aging tests vs field performance of PV modules, Prog. Energy. 4 (2022) 42009. https://doi.org/10.1088/2516-1083/ac890a.